Available online at www.sciencedirect.com
SCIENCE DIRECT®
Catalysis Today 89 (2004) 5–14
CATALYSIS TODAY
www.elsevier.com/locate/cattod

Plasma catalytic hybrid processes: gas discharge initiation and plasma activation of catalytic processes

Th. Hammer*, Th. Kappes, M. Baldauf

Siemens AG, Corporate Technology, CT EN3, Paul-Gossen-Str. 100, 91052 Erlangen, Germany

Abstract

Catalytic reactions of a gas mixture can efficiently be induced by pre-treatment using a gas discharge plasma or by combined treatment in a plasma catalytic hybrid reactor. The effects of plasma treatment can be excitation of molecules, formation of short lived radicals, formation of long lived intermediate species, emission of UV-radiation, or simply gas heating.

By dielectric barrier discharge (DBD) pre-treatment of Diesel engine exhaust selective catalytic reduction (SCR) of nitric oxides on a V_2O_5-WO_3/TiO_2-catalyst could be induced at temperatures as low as 100 °C. Due to the low specific plasma input energy density ε_{sp} of about 10 J/l gas heating does not play a role. Plasma catalytic methane steam reforming using a Ni-catalyst was performed in a dielectric packed bed reactor at temperatures down to 200 °C. Since for reforming ε_{sp} values exceed 1 kJ/l both non-thermal plasma effects and gas heating contribute to the plasma catalytic hybrid process. A review focusing on the plasma-chemical kinetics is given.

Keywords: Plasma catalytic; Catalyst; Dielectric barrier discharge; Dielectric packed bed reactor; Streamer breakdown; Selective catalytic reduction; Nitric oxides; Steam reforming; Methane; UV-radiation; Electron collision dissociation; Electronic excitation; Vibrational excitation; Thermal activation

1. Introduction

Plasma processes offer a unique way to induce gas phase reactions. Arcs are utilized for thermal activation of fast conversion processes [1] like acetylene generation from natural gas, dielectric barrier discharges (DBDs) for the non-thermal activation of low temperature processes [2] like ozone generation. However, plasma processes are not always selective. Catalytic processes on the other hand can be very selective but often require a certain gas composition and a sufficiently high temperature [3].

Examples are the NO_x reduction using CO and hydrocarbons on a three way catalyst requiring a nearly oxygen free atmosphere and an activation temperature of about 220–250 °C. In an oxidizing atmosphere NO_x reduction requires a special reducing agent like NH_3.

To combine the unique way of plasma activation of reactions with the selectivity of catalytic reactions plasma catalytic hybrid processes have been investigated. Examples of such hybrid processes are plasma enhanced selective catalytic reduction (SCR) and reforming of methane to hydrogen and higher hydrocarbons. In this paper, a review of plasma processes inducing catalytic reactions will be given. The numerical simulation of non-thermal plasma chemical kinetics induced by dielectric barrier discharges will be presented in detail. These efforts do not only cover the simulation of spatially homogeneous gas discharges coupled to chemical reactions but also includes gas discharge ignition in inhomogeneous electrical fields. In addition important questions like gas heating, side reactions, and adsorption processes are addressed in this review.

2. Plasma activation of catalytic processes

At atmospheric gas pressure catalytic processes may be induced by different plasma activation mechanism: First of all the plasma may simply cause gas heating, vibrational excitation, and dissociation of molecules. Due to electronic and ionic collision processes dissociation of molecules and heating proceed much faster than in any conventional heat exchanger. Thus in a compact reactor near thermal degrees of dissociation may be achieved if a plasma with high specific input energy density is applied to the flowing gas. However, in spite of strong gas heating the plasma may be far from being thermal: The average electron energy can be

* Corresponding author. Tel.: +49-9131-7-34870; fax: +49-9131-7-24709.
E-mail address: thomas.hammer@siemens.com (Th. Hammer).

0920-5861/$ – see front matter © 2003 Elsevier B.V. All rights reserved.
doi:10.1016/j.cattod.2003.11.001

substantially above 1 eV whereas the gas temperature is in the range of several hundred degrees Celsius only. Examples of gas heating effects can be found in the reformation of methane to hydrogen, CO, and higher hydrocarbons by application of a μ-plasmatron discharge and a Ni-catalyst [4]. Another example is the dielectric barrier discharge induced reforming of methane to hydrogen and higher hydrocarbons [5,6].

When in a DBD-reactor or in a pulsed corona discharge (PCD) reactor the specific input energy density is reduced to values below 100 J/l gas heating effects get more and more unimportant. Depending on the gas mixture a specific input energy density of 10 J/l corresponds to a gas temperature increase of roughly 10–15 °C. Under these conditions average electron energies may be as high as 5 eV, and efficient ionization and dissociation of molecules occurs, whereas vibrational excitation gets more and more unimportant.

In order to have an influence of radical formation on catalytic reactions the radical formation has to take place near the catalyst surface. A reactor concept working in this way is the dielectric packed bed (DPB) reactor [7], where high electric fields cause plasma generation near to the surface of the dielectric packing, which may be a catalyst itself or may have a catalytic coating. A restriction of this reactor concept is that the electrical conductivity of the catalyst has to be low.

The plasma may generate intermediate species having a sufficiently long lifetime to induce reactions on a catalyst placed flow-down of the plasma reactor. An example is plasma enhanced selective catalytic reduction of nitric oxides in the exhaust gases of internal combustion engines. By plasma pre-treatment NO is converted to NO_2, which enables the reduction on a V_2O_5-WO_3/TiO_2-catalyst to be performed at a lower temperature when NH_3 is used as a reducing agent [8,9]. Further from unburned hydrocarbons aldehydes are generated [10]. This in turn enables NO_x reduction on catalysts like NaY-zeolite or γ-Al_2O_3 using hydrocarbons as a reducing agent. Because of catalytic oxidation of the hydrocarbons by molecular oxygen, however, the selectivity of hydrocarbons towards NO_x reduction is much lower than that of NH_3 on a SCR-catalyst.

At reduced pressure the lifetime of radicals formed in a plasma reactor may be long enough to allow plasma induced catalytic reactions even for a catalyst placed flow-down of the plasma reactor [11]. In addition in this case higher average electron energies can be achieved because at lower values of the reduced discharge gap with $n{\cdot}d$ discharge ignition takes place at higher reduced electric field strength E/n. The electron energy distribution and thus the average electron energy depends on the reduced electric field and on the gas composition. The formation of NH_3 from N_2 and H_2 is an example both of the high average electron energy allowing excitation or even dissociation of nitrogen and of the plasma catalytic hybrid process induced thereby.

Finally the plasma may be a source of ultraviolet radiation [12], which enables photo-catalytic reactions. A catalyst successfully used for oxidative and reductive photo-catalytic degradation of pollutants in industrial process water is anatase TiO_2 (see [13] and references therein). Photo-catalytic oxidation of volatile organic compounds in air has also been investigated [14]. However, in all these cases UV-radiation has been supplied by an external light source. In recent investigations DBDs were combined directly with photo-catalysts [15].

In the following chapter non-thermal plasma generation and non-thermal plasma induced chemical reactions shall be described step by step. Finally one example of plasma induced processes on a catalyst surface is given.

3. Gas discharge ignition

For the practical application of non-thermal plasma methods the ignition voltage is an important design parameter of the gas discharge reactor. Therefore in a first step a short overview of breakdown mechanisms shall be given, where for simplicity the electric field is assumed to be homogeneous and formation of negative ions, chemo-ionization, and Penning-ionization are not taken into account. For a more detailed treatment the interested reader is referred to textbooks [16]. Then a streamer breakdown model is presented which allows to estimated the streamer breakdown voltage of an arbitrary electrode geometry.

3.1. Townsend breakdown mechanism

At sufficiently low values of the gas density n and the discharge gap d the breakdown can be described by the Townsend mechanism: A single electron released from the cathode generates an electron avalanche growing exponentially on the way to the anode. This growth is characterized by the ionization coefficient α (first Townsend coefficient) which depends on the electric field E, the gas density n, and on the gas composition represented by the molar fractions of the gas components c_k:

$$\frac{\alpha}{n} = f\left(\frac{E}{n}, c_k\right) \tag{1}$$

From this electron avalanche secondary electrons are released from the cathode by feedback mechanisms like drift and diffusion of positive ions or metastable molecules to the cathode or photo effect due to UV-irradiation. The probability of secondary electron emission due to these feedback mechanisms is described by γ (second Townsend coefficient) which is the ratio of the number of electrons released to the number of electrons accumulated in the avalanche on the way to the anode. Discharge ignition occurs if in one cycle for every electron starting from the cathode at least one secondary electron is released from the cathode. This breakdown mechanism is described by Paschen's law:

$$\gamma(e^{\alpha d} - 1) = 1 \tag{2}$$

Combining (1) and (2) one finds that the reduced breakdown field E/n is a function of the reduced discharge gap $n{\cdot}d$, the gas composition, and the probability for secondary electron emission from the cathode:

$$\alpha \cdot d = \ln\left(1 + \frac{1}{\gamma}\right) = f\left(\frac{E}{n}, c_k\right)(n \cdot d) \tag{3}$$

The second Townsend coefficient, however, may vary for orders of magnitude depending on the microscopic properties of the cathode surface and the gas mixture.

3.2. Streamer breakdown mechanism

When the reduced discharge gap $n{\cdot}d$ is increased to values of the order of $10^{22}\,\mathrm{m}^{-2}$ gas discharge ignition can occur at reduced fields E/n lower than those predicted by Paschen's law. Under these conditions dielectric breakdown is no longer described by the Townsend mechanism but by the streamer mechanism. It's basic idea is that at large reduced discharge gaps a single avalanche can accumulate enough electrons in the avalanche head to distort the externally applied electric field. Due to the field distortion the avalanche formation is accelerated. When the electric field generated by the space charges exceeds the externally applied field gas discharge breakdown is assumed to take place. There are sophisticated models for the numerical simulation of streamer breakdown phenomena solving the Poisson equation coupled to the continuity equations of electrons and ions. However, even in the case of simplifying assumptions like rotational symmetry, constant radius of the streamer channel, and a very limited reaction kinetic model these simulations require large amounts of CPU time. Therefore for practical application a simplified approach may be preferred:

In a homogeneous electric field Raether's criterion gives a good approximation of the reduced breakdown field:

$$\alpha \cdot d = \ln\left[\frac{16\pi \cdot \varepsilon_0}{e_0}\frac{n \cdot D_\mathrm{e}}{v_\mathrm{drift}}\frac{E}{n}d\right] \approx -\mathrm{const} + \ln(d) \tag{4}$$

where ε_0 is the vacuum permittivity, e_0 the elementary charge, v_drift the electron drift velocity, and D_e the electron diffusion coefficient. If the discharge gap d is given in units of meters the constant typically takes a value of 23.

3.3. Streamer breakdown in inhomogeneous electric fields

In the case of an inhomogeneous electric field, e.g. generated by a pin-to-plane electrode arrangement the avalanche growth will proceed along an electric field line represented by a path s [17]. The electrode voltage V is related to the externally applied electric field along s by

$$V = \int_0^d E(s)\,\mathrm{d}s \tag{5}$$

Breakdown is assumed to occur if somewhere in the discharge gap the electric field generated by the space charge exceeds the externally applied field:

$$\frac{e_0}{4\pi \cdot \varepsilon_0}\frac{\exp\left\{\int_0^\xi \alpha_\mathrm{eff}(\mathrm{s})\,\mathrm{d}s\right\}}{4\int_0^\xi (D_\mathrm{e}(s)/v_\mathrm{drift}(s))\,\mathrm{d}s} > E(\xi) \tag{6}$$

In this relation the loss of electrons due to dissociative attachment is taken into account using the effective ionization coefficient α_eff. In order to solve this implicit equation for the streamer breakdown voltage the coefficients α_eff, v_drift, and D_e have to be known as a function of E/n. For pure gases and some gas mixtures like dry air tabulations of these values can be found in the literature [18,19]. For arbitrary gas mixtures they can be calculated from the electron collision cross-sections of the molecules and the electron energy distribution function which for not too high E/n values can readily be achieved by a numerical solution of the Boltzmann equation in two-term approximation [20]. In this case the tabulations of the coefficients for pure gases can be utilized to validate the numerical simulations.

As an example in Fig. 1 the electric field distribution inside of a coaxial DBD-reactor containing sharp edged discs as a HV-electrode obtained by electrostatic field simulation [21] is given.

In Diesel exhaust which is simulated by a gas mixture containing 13.7% O_2, 4.5% CO_2, 5.3% H_2O, 76.5% N_2 this electrode design results in a breakdown voltage of 8.8 kV (Fig. 2) which is in good agreement with the experimental value of 7.9 kV measured under repetitive pulsed excitation

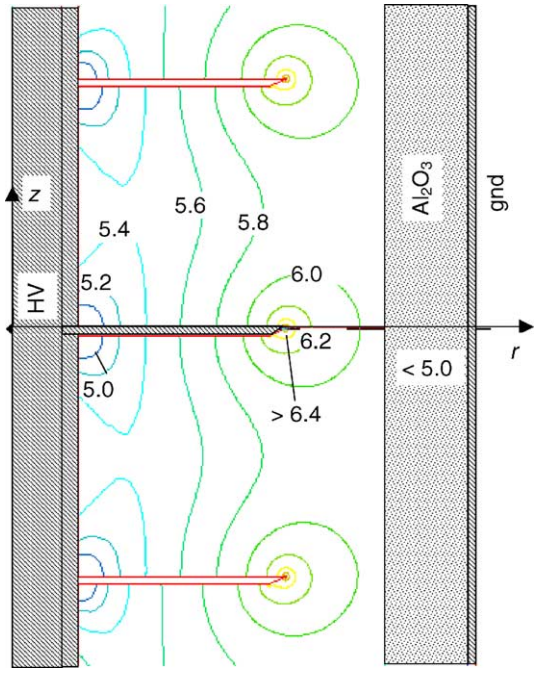

Fig. 1. Electric field distribution $\log(E(\mathrm{V/m}))$ of a coaxial DBD-reactor consisting of sharp edged discs used as HV-electrodes, a 5 mm thick alumina barrier (relative permittivity 9.2), and the ground electrode coated on the outer barrier surface. The discharge gap is 6 mm, the applied voltage 10 kV.

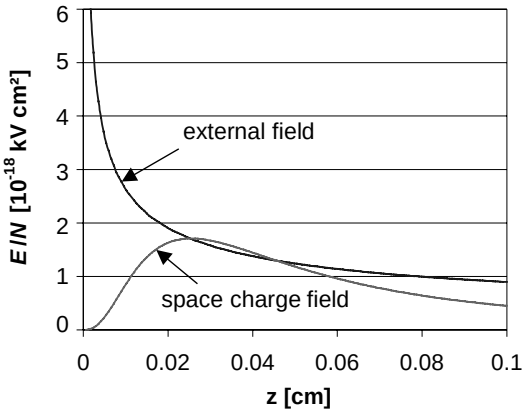

Fig. 2. Electric field distribution calculated for the breakdown voltage of 8.8 kV (discharge gap 6 mm, synthetic Diesel exhaust (13.7% O_2, 4.5% CO_2, 5.3% H_2O, 76.5% N_2 at 212 °C)).

of the DBD-reactor. For a homogeneous electric field a streamer breakdown voltage of 15.6 kV is calculated.

Because at constant pressure p the gas density n is a function of the temperature T,

$$p = n \cdot k_B \cdot T \tag{7}$$

where k_B is the Boltzmann constant, relation (6) can be utilized to evaluate the temperature dependency of the streamer breakdown voltage.

4. Gas discharge induced chemical reactions

In an electrical gas discharge chemical reactions are induced by electron collision processes such as ionization, dissociation, and electronic excitation. From the numerical simulations mentioned above not only the effective ionization coefficient but rate coefficients as a function of E/n for electron collision processes other than ionization and attachment can be obtained, too. Therefore gas discharge induced chemical processes can be taken into account in the numerical simulation of chemical kinetics by including the corresponding reaction equations and rate coefficients into the kinetic model. However, a problem arises from the inhomogeneous electric field which in addition changes rapidly during streamer breakdown. Nevertheless, from a sophisticated two-dimensional gas discharge simulation coupled to a reactive flow simulation excellent agreement with experiments on dielectric barrier discharge treatment of Diesel exhaust could be obtained [22,23]. Of course a simple zero-dimensional approach assuming a homogeneous gas discharge is much more convenient and often results in a reasonable agreement with experimental results.

In the following sections results are reported which were obtained using such a zero-dimensional discharge model consisting of an electrical circuit model for the calculation of electrical voltages and currents, a Boltzmann solver for the calculation of electron drift velocity, diffusion coefficient, and reaction rate coefficients of electron collision reactions, a streamer breakdown model for a homogeneous electric field, and a rate equation solver for the calculation of species concentrations [24]. When electrode structures generating inhomogeneous electric fields were used in this model the discharge gap is chosen such that the simulated breakdown voltage fits the measured one.

4.1. Diesel exhaust after-treatment

For the simulation of DBDs in Diesel exhaust a reaction kinetic model similar to those published, e.g. by Penetrante and co-workers has been used [25]. A detailed listing of the reactions and rate coefficients taken into account can be found elsewhere [26,27].

In order to fit the measured streamer breakdown voltage the coaxial DBD-reactor with the structured HV-electrode shown in Fig. 1 was simulated by a parallel plate reactor having a discharge gap of 3 mm. Since in the experiments a pulse voltage source with a voltage pulse duration of about 1 s was used a voltage rise rate of 20 kV/μs was assumed in the model. The electrical signals resulting from a single DBD-filament are shown in Fig. 3. Until streamer breakdown the average electron energy rises up to 5 eV. After streamer breakdown due to surface charging the gap voltage and the average electron energy drop for about 50% and the discharge extinguishes. Thereby the current pulse duration is limited to some 10 ns.

In the early discharge phase radicals are generated (Fig. 4). Because the dissociation energy of O_2 is low compared to that of N_2, in Diesel- and lean burn gasoline engine exhausts having oxygen concentrations of several percents the oxygen dissociation

$$e + O_2 \rightarrow e + O + O \tag{8}$$

is the most important radical formation reaction. Due to their high reactivity atomic nitrogen (N), electronically

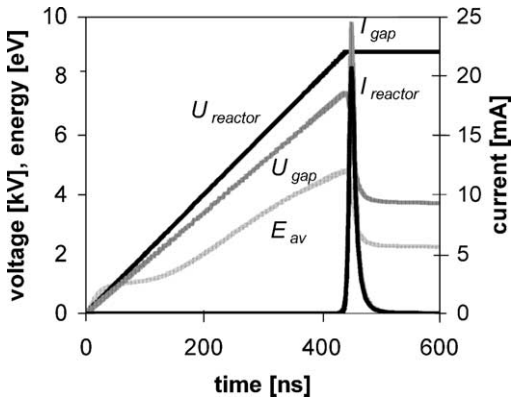

Fig. 3. Voltages, currents, and mean electron energy of the DBD-reactor. $U_{reactor}$, $I_{reactor}$—outer voltage and current; U_{gap}, I_{gap}—voltage and current at the discharge gap; E_{av}—average electron energy. Synthetic Diesel exhaust (13.7% O_2, 4.5% CO_2, 5.3% H_2O, 76.5% N_2, and 450 ppm NO at 212 °C).

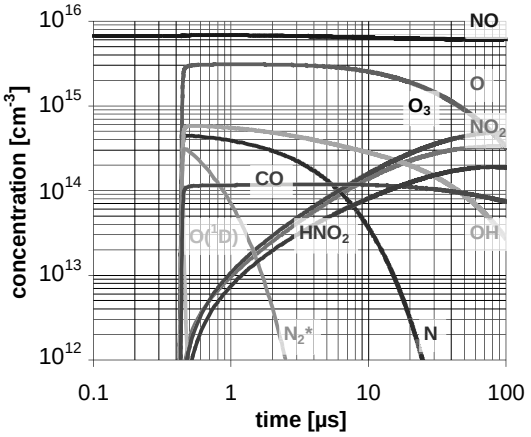

Fig. 4. DBD induced radical formation and conversion of gaseous compounds in synthetic Diesel exhaust (13.7% O_2, 4.5% CO_2, 5.3% H_2O, 76.5% N_2, and 450 ppm NO at 212 °C).

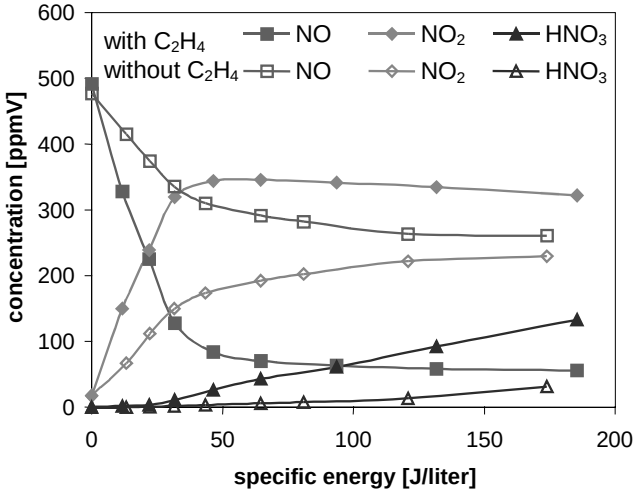

Fig. 5. Influence of ethylene on the conversion of NO in a coaxial DBD-reactor with a structured HV-electrode, discharge gap 4 mm, and sinusoidal excitation, frequency 1 kHz (synthetic gas mixture: 72% N_2, 18% O_2, 10% H_2O, 500 ppm NO, 500 ppm C_2H_4, gas temperature 200 °C).

excited nitrogen (N_2*), and electronically excited atomic oxygen ($O(^1D)$) are very short-lived radicals, whereas ground state atomic oxygen (O) and hydroxyl (OH) have a longer lifetime. Depending on the temperature nitrogen radicals reduce nitric oxide NO (low temperature) or form new NO in reactions with O_2 (high temperature). $O(^1D)$ reacts with water resulting in formation of OH radicals. O- and OH-radicals are removed by formation of ozone (O_3), oxidation of NO to NO_2, HNO_2, and HNO_3, which limits their lifetime to about 100 μs. Therefore unless such radicals are generated very near to a catalytic surface it is unlikely that at atmospheric pressure gas discharges induce catalytic reactions via radical generation. Nevertheless plasma assisted catalytic reactions were observed not only in a one-stage DPB plasma catalytic hybrid reactor but in a two-stage reactor consisting of a DBD-reactor flow-up of a catalytic reactor [8,28–31]. Due to the high average electron energy vibrational excitation contributes to the energy balance for less than 25%, only. Further ions do not contribute substantially to the conversion of noxious compounds. When hydrocarbons are added to the gas mixture the kinetic model has to be extended [32]. In experiments with gas mixtures containing ethylene as an additive an improved conversion of NO to NO_2 and HNO_3 was observed (Fig. 5). This effect is caused by the formation of peroxy radicals R–OO, which promotes the oxidation of NO to NO_2 and suppresses the back reaction of NO_2 to NO [33,34]. Therefore in Diesel exhaust the presence of unburned hydrocarbons reduces the energy requirements for the conversion of NO to NO_2 [35]. Formaldehyde turns out to be an important intermediate compound of ethylene conversion to CO and CO_2 (Fig. 6). Similar effects are observed with hydrocarbons like propene, propane, *n*-octane, and dodecane [29,36–39].

The specific energy requirements for the oxidation of noxious compounds like NO in Diesel exhaust are roughly proportional to the amount converted. For an initial NO-concentration of 500 ppmv about 15 J/l are required for a conversion of 50% [40]. Therefore energy losses due to gas heating can be neglected.

4.2. Plasma reforming of methane

Depending on the gas mixture plasma reforming of methane may be initiated by different reactions. Applying numerical simulation to methane steam reforming we found that for a gas mixture consisting of 33% CH_4 and 66% H_2O the most important reaction is the dissociation of methane [41]

$$e + CH_4 \rightarrow e + CH_3 + H \quad (9)$$

With respect to the energy branching in electron collisions this may, however, not be the dominating reaction: At a reduced electric field strength of 100 Td (1 Td = 10–21 V m^2) about 60% of the electron energy is spent for vibrational excitation of water, whereas 25% are utilized for dissociation

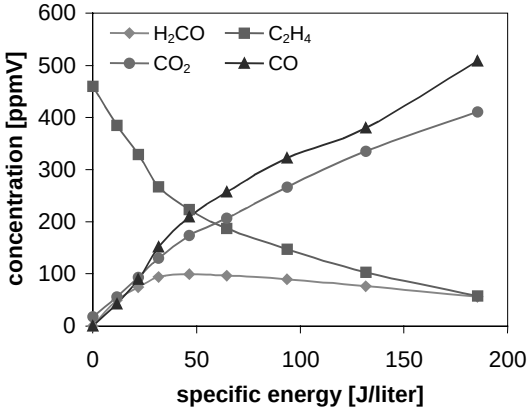

Fig. 6. Conversion of ethylene in a coaxial DBD-reactor (experimental conditions see Fig. 5).

of CH_4, only [41]. When the reduced electric field strength is increased to 200 Td as much as 50% of the energy may be spent for CH_4-dissociation, whereas still less than 10% of the energy are spent for water ionization and dissociation by electron collisions.

In addition at a gas temperature of 400 °C about 80% of the H- and CH_3-radicals are lost in recombination reactions forming CH_4 again:

$$CH_3 + H \rightarrow CH_4 \quad (10)$$

The remaining H-radicals generate molecular hydrogen by H-abstraction from CH_4

$$H + CH_4 \rightarrow H_2 + CH_3 \quad (11)$$

and 75% of the remaining CH_3-radicals contribute to the formation of C_2H_6

$$CH_3 + CH_3 \rightarrow C_2H_6 \quad (12)$$

In total about 8% of the input energy is spent for H_2-generation. This simple mechanism explains both the reaction products and the energy costs for methane conversion and hydrogen generation by DBD induced steam reforming observed experimentally in the temperature range of 200–600 °C (Fig. 7) [41]: The low yield of oxygenated compounds clearly indicates that either the H_2O is not dissociated or H_2O dissociation is foiled by recombination of the dissociation products. From the numerical simulation of the input energy branching a fraction of less than 5% was obtained for H_2O dissociation. Therefore the main reason for low yield of oxygenates is assumed to be insufficient plasma activation of steam. However, there is evidence from kinetic simulation that a substantial fraction (61%) of the OH-radicals generated by H_2O-dissociation is consumed by H-abstraction from CH_4 resulting in the generation of a CH_3-radical and H_2O, whereas only 29% of the OH-radicals are consumed for the formation of methanol.

The increase of the CH_4 conversion efficiency as well as the increase of the yields of H_2 and C_2H_6 with increasing temperature can be explained by the temperature dependency of the rate coefficients of reactions (9)–(12). Between 200 and 600 °C the rate coefficients for methyl formation due to electron collision dissociation (9) and hydrogen abstraction (11) increase for a factor of 1.4 and 316, respectively, whereas the rate coefficients for methyl quenching (10) and methyl–methyl recombination (12) decrease for a factor of 3 and 20, respectively.

5. DBD induced heating

Because of the high concentrations of the compounds to be converted the conditions that apply for plasma reforming are completely different from those of plasma exhaust gas after-treatment. Therefore even in the case of non-thermal plasma treatment, e.g. using DBD-reactors or DPB-reactors it is important to check the energy balance for thermal effects like gas heating [42,43]. A simple thermodynamic consideration of the temperature as a function of additional enthalpy input shows that gas heating caused by DBD-treatment may not be neglected (Fig. 8).

Indeed in experimental investigations the observation was made that the electric power required for heating the reactor to keep the temperature at the desired level decreased when the plasma input power was increased. Therefore experiments were performed where the reactor was not heated electrically but preheated gas was flowing into the DBD-reactor isolated thermally by four layers of ceramic wool á 1 cm. Under these conditions due to thermal losses the gas cooled down from an inlet temperature of about 380 °C to an outlet temperature of about 240 °C as long as there was no plasma excitation (Fig. 9). When the DBD plasma was switched on (average reactor input power 180 W) the barrier temperature increased rapidly (12 K/min) in regions with discharge activity (barrier 2), whereas the barrier temperature in regions without discharge activity (barrier 1 and barrier 3) increased

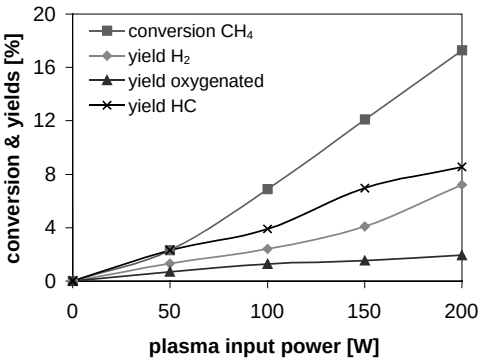

Fig. 7. Conversion and yields of DBD induced methane steam reforming at 200 °C as a function of the plasma power (gas mixture 33% CH_4, 67% H_2O, gas flow 1 l (STP)/min, pre-heated to 200 °C). The reactor temperature is controlled thermostatically.

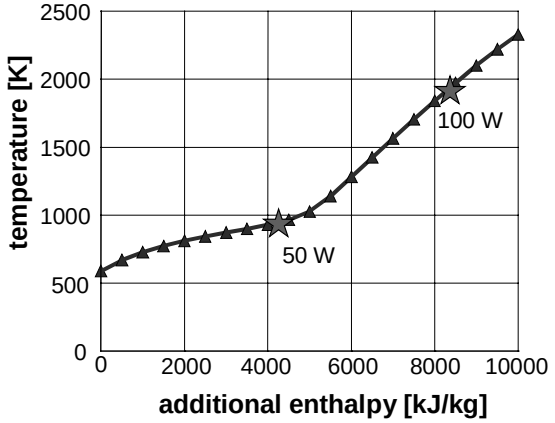

Fig. 8. Temperature as a function of additional enthalpy for a 1:2 mixture of CH_4 and H_2O, initial temperature 400 °C. The stars mark the additional enthalpy corresponding to plasma input powers of 50 and 100 W, respectively, at a gas flow of 1 l (STP)/min.

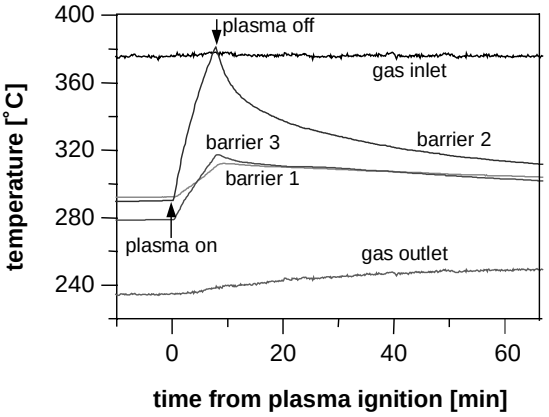

Fig. 9. Influence of the plasma excitation on gas and barrier temperatures of a DBD-reactor treating a gas flow of 3 l (STP)/min at an average reactor input power of 180 W.

slowly (<5 K/min). The outlet gas temperature did not increase substantially. An energy balance was performed which indicated that 63% of the average reactor input power was spent for barrier heating. The barrier heating may be caused by losses inside of the alumina barrier or by energy transfer from the footprints of the DBD-filaments to the barrier: It is well known that for ceramic materials polarization losses as well as ohmic losses due to ionic conductivity increase for orders of magnitude when the temperature is increased [44]. Therefore it is a reasonable assumption that a fraction of the observed barrier heating is due to barrier losses. On the other hand vibrational excited species can have a long lifetime of the order of milliseconds, and ionic species may have a long lifetime, too. Thus barrier heating can be caused by vibrational de-excitation and ionic or electronic recombination processes taking place at the barrier surface. Since in the footprint area of a DBD-filament a substantial fraction of the discharge energy is dissipated, e.g. by vibrational excitation of H_2O these processes can be responsible for barrier heating as well. However, the polarization losses and the ohmic losses of the barrier material increase with increasing electric field strength inside of the barrier. In regions where no gas discharge action occurs the electric field strength inside of the Al_2O_3 barrier is about one order of magnitude lower than in the discharge gap. On the other hand due to discharge filaments bridging the discharge gap the barrier capacity is charged locally resulting in an increase of the electric field inside of the barrier material for an order of magnitude. Therefore independent of the mechanism barrier heating is strongly coupled to the occurrence of discharge filaments. In order to find the main reason for barrier heating additional investigations are desirable.

6. Plasma assisted catalytic NO_x reduction in the exhaust of lean combustion engines

As already mentioned above, by plasma treatment oxidation reactions of NO and hydrocarbons are induced in Diesel exhaust. In cooperation with DaimlerChrysler experiments were performed in our laboratory [39] where synthetic gas mixtures containing 82% N_2, 8% O_2, 10% H_2O, 113 ppm dodecane, and 270 ppm NO, respectively, were first pre-treated in a DBD-reactor energized by a pulse voltage source at a specific energy density of 16 J/l and then reacted on a lean NO_x catalyst (Ag doped γ-Al_2O_3) with a

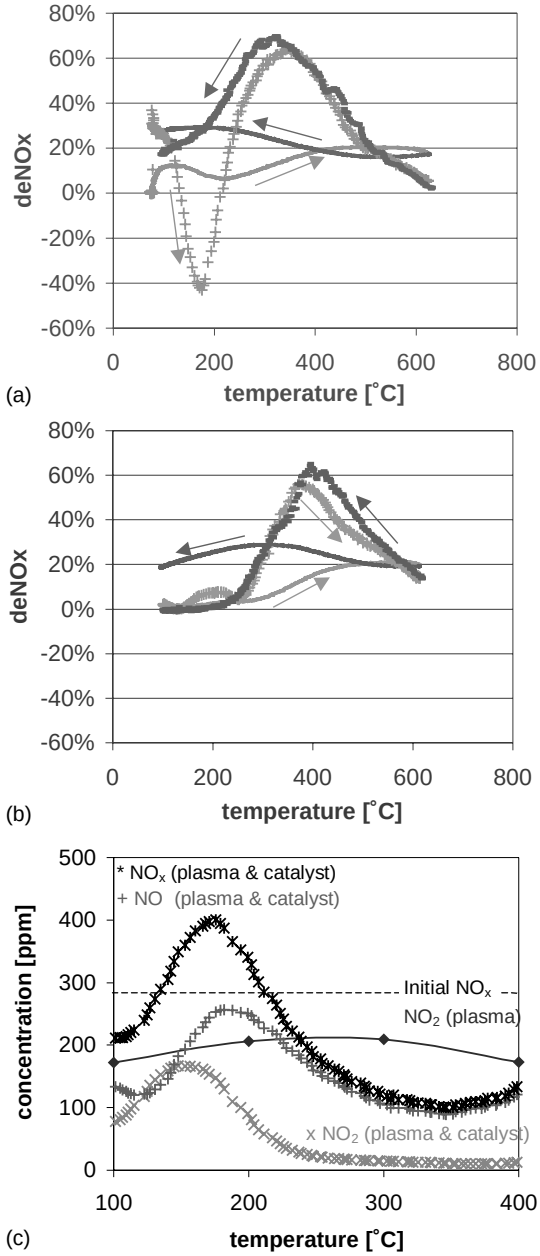

Fig. 10. (a) Plasma catalytic removal of NO_x from a synthetic exhaust gas observed in temperature cycling experiments. Symbols represent instantaneous NO_x-removal, full lines cumulative removal. The arrows indicate the direction of temperature change. (b) For comparison catalytic NO_x-removal (without plasma pre-treatment) is shown. (c) Instantaneous plasma catalytic NO-, NO_2-, and total NO_x-removal observed during the heating phase. For comparison the NO_2-concentration after plasma treatment is shown.

normalized space velocity of 50,000 h^{-1}. The reaction chain desired for this hybrid process of course is

$NO,\ C_{12}H_{26}$

→ plasma induced intermediate product formation

→ catalytic reduction of NO to N_2, H_2O, CO_2

In order to investigate adsorption- and desorption processes, after constant operation at about 100 °C for some minutes a temperature ramp of 10 K/min ending at 600 °C was applied, which was followed by 10 min of constant operation at 600 °C and a negative temperature ramp of −20 K/min down to 100 °C again. This temperature cycle was repeated at least two times in order to see if the results are reproducible. The complexity of plasma induced catalytic processes can be seen from Fig. 10a–c: Without plasma pre-treatment NO_x-removal was observed for $T > 250$ °C (Fig. 10b). Differences between ramp-up and ramp-down were due to hydrocarbon adsorption and desorption processes. With plasma pre-treatment NO_x-removal was observed at lower temperatures, too (Fig. 10a). In more detail (Fig. 10c), at temperatures below 130 °C about 50% of the NO_2 formed by plasma pre-treatment is removed from the gas mixture. This removal is partly caused by catalytic reduction to NO, however, as can be seen from comparison with runs performed without plasma pre-treatment, it is partly caused by adsorption on the catalyst surface, too. When the temperature is increased, NO desorption occurs and the NO-concentration runs through a maximum at about 180 °C. This indicates, that at temperatures below 180 °C no NO_x-reduction to N_2 takes place at all.

Similar adsorption- and desorption processes concurring with catalytic oxidation reactions were observed for hydrocarbons. The hydrocarbon emission and the CO emission were substantially higher for increasing than for decreasing temperature. Adsorption–desorption processes as well as partial oxidation of the hydrocarbon were strongly influenced by plasma pre-treatment: During temperature rise CO-emission at 200 °C, e.g. was increased from about 20–122 ppm due to the DBD-treatment.

In summary for the investigation of plasma catalytic hybrid processes care has to be taken to detect unwanted side-reactions as well as adsorption processes, which both may both be confused with the desired reaction.

7. Plasma catalytic hybrid reforming of methane

Plasma catalytic hybrid reforming of a CH_4–H_2O mixture with a molar ratio of 1:2 was performed in a dielectric packed bed reactor consisting of an alumina tube as a dielectric barrier, a cylindrical high voltage electrode inside of that tube, and a metallic coating of the outer surface of the alumina tube serving as a ground electrode. The discharge gap was filled with a Ni-catalyst which was dispersed on ceramic pellets having a diameter of 2–4 mm. For electrical excitation a sinusoidal voltage with a frequency in the 10 kHz range and a maximum power of 600 W was applied. The experiments were performed under thermostatically controlled conditions in the temperature range of 200–600 °C. Compared to the DBD reforming described above a much better conversion of methane and especially of steam was observed [45]. A more detailed look at the experimental results (Fig. 11) shows, that due to plasma treatment the CO_2-selectivity is reduced. For temperatures below 400 °C this is a clear indication of non-thermal plasma effects, for temperatures above 400 °C, however, this may be caused by gas heating, too: At low temperatures the exothermic water shift reaction

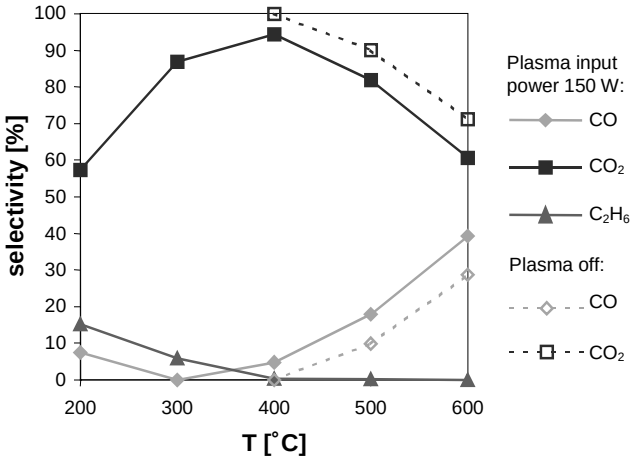

Fig. 11. Influence of the plasma treatment on the product selectivity of catalytic methane steam reforming on a commercial Ni-catalyst. The CH_4–H_2O-ratio was 1:2, the gas flow rate 1 l (STP)/min, the plasma input power 150 W.

$$CO + H_2O \rightarrow CO_2 + H_2 \quad (13)$$

is favored, whereas at increased temperature formation of CO_2 is not favorable due to thermodynamic reasons.

Heating may be caused from dielectric losses of the catalyst bed, from ohmic heating at the contact points of the pellets in the catalyst bed, and from energy transfer of the gas discharge to the catalyst.

8. Summary and conclusions

Numerical simulation has been shown to be a valuable tool for the investigation of plasma catalytic hybrid processes as well as for the development of gas discharge reactors and electrical power supplies.

In order to assist the design of atmospheric pressure gas discharge reactors and electrical power supplies the combination of electrostatic field simulation with a gas discharge breakdown model can be utilized to predict ignition voltages.

In conjunction with experimental results the combination of a simple gas discharge model and a reaction kinetic

model can be applied to identify the most important chemical reactions as well as unwanted side reactions. Based on these results the energy balance can be evaluated, trends can be predicted, and the potential of the plasma-chemical process for practical application can be estimated. Further the simulation gives information on concentrations and lifetimes of intermediate products formed in the gas discharge which can be utilized to identify plasma induced catalytic reactions.

From thermal equilibrium simulation product gas composition limits of catalytic reactions as well as rough estimations of the gas heating and/or the thermal energy losses of plasma treatment can be obtained.

Recently, a lot of atmospheric pressure plasma catalytic hybrid processes have been identified. Non-thermal plasma effects induced, e.g. by radical formation are playing an important role for applications where only low specific energy densities are required like automotive exhaust gas treatment or removal of volatile organic compounds from off-gases. In processes requiring a high specific energy density the role of the plasma is not always clear: Both gas heating and non-thermal plasma induced processes like radical formation, ionization or vibrational excitation may be important. More investigations are required to answer this question.

Because of the complexity of plasma catalytic hybrid systems special care has to be taken to distinguish plasma induced adsorption- and desorption processes on the catalyst surface as well as unwanted side reactions from the desired reaction. The investigation of this important issue is just at its beginning.

References

[1] M.I. Boulos, P. Fauchais, E. Pfender, Thermal Plasmas: Fundamentals and Applications, vol. 1, Plenum Press, New York, 1994.
[2] B. Eliasson, Ulrich Kogelschatz, IEEE Trans. Plasma Sci. 19 (6) (1991) 1063–1077.
[3] E.S.J. Lox, B.H. Engler, in: G. Ertl, H. Knözinger, J. Weitkamp (Eds.), Environmental Catalysis, Wiley-VCH, Weinheim, 1999, pp. 1–117.
[4] L. Bromberg, D.R. Cohn, A. Rabinovich, N. Alexeev, Int. J. Hydrogen Energy 24 (12) (1999) 1131–1137.
[5] B. Eliasson, C.-J. Liu, U. Kogelschatz, Ind. Eng. Chem. Res. 39 (5) (2000) 1221–1227.
[6] T. Nozaki, Y. Unno, Y. Miyazaki, K. Okazaki, J. Phys. D: Appl. Phys. 34 (16) (2001) 2504–2511.
[7] J.M. Henis, US Patent 3,983,021 (1976).
[8] Th. Hammer, S. Broer, in: Society of Automotive Engineers, Plasma Exhaust Aftertreatment, Special Publication SP-1395, 1998, pp. 7–12.
[9] S. Bröer, Th. Hammer, Appl. Catal. B: Environ: 28 (2000) 101–111.
[10] S. Yoon, A.G. Panov, R.G. Tonkyn, A.C. Ebeling, S.E. Barlow, M.L. Balmer, Catal. Today 72 (2002) 243–250.
[11] S. Veprek, M. Venugopalan, Kinetics and catalysis in plasma chemistry. Plasma chemistry IV. Topics in Current Chemistry, vol. 107, Springer-Verlag Berlin, Heidelberg, New York, 1983, pp. 3–58.
[12] B. Gellert, U. Kogelschatz, Appl. Phys. B 52 (1991) 14–21.
[13] M. Hilgendorff, M. Hilgendorff, D.W. Bahnemann, J. Adv. Oxid. Technol. 1 (1) (1996) 35–43.
[14] R.M. Alberici, W.F. Jardim, J. Adv. Oxid. Technol. 3 (2) (1998) 182–187.
[15] H.H. Kim, K. Tsunoda, S. Katsura, A. Mizuno, IEEE Trans. Ind. Appl. 35 (6) (1999) 1306–1310.
[16] J. Dutton, in: J.M. Meek, J.D. Craggs (Eds.), Electric Breakdown of Gases, Wiley Series in Plasma Physics, Wiley, New York, 1978, pp. 209–318.
[17] R.T. Waters, in: J.M. Meek, J.D. Craggs (Eds.), Electric Breakdown of Gases, Wiley Series in Plasma Physics, Wiley, New York, 1978, pp. 385–532.
[18] J. Dutton, J. Phys. Chem. Ref. Data 4 (3) (1975) 577.
[19] J.W. Gallagher, E.C. Beaty, J. Dutton, L.C. Pitchford, J. Phys. Chem. Ref. Data 12 (1) (1983) 109.
[20] Kinetic Technologies (KINTECH): Chemical WorkBench version 2.5, Moscow, 2000.
[21] Maxwell 2D Version 9, Ansoft Corporation, 2002.
[22] R. Wegst, M. Neiger, H. Russ, S. Liu, SAE paper no. 1999-01-3686 (1999).
[23] I. Orlandini, U. Riedel, J. Phys. D: Appl. Phys. 33 (2000) 2467–2474.
[24] H. Müller, Modellierung von Excimer-Gasentladungen zur Erzeugung spektral selektiver Strahlung, Doctoral Thesis, Faculty of Electrical Engineering, University Karlsruhe, Germany, 1991, 300 pp.
[25] C.R. McLarnon, B.M. Penetrante, in: Society of Automotive Engineers, Plasma Exhaust Aftertreatment, Special Publication SP-1395, 1998, pp. 37–48.
[26] M. Klein, Barrierenentladungen zur Entstickung motorischer Abgase, Doctoral Thesis, Faculty of Electrical Engineering, University Karlsruhe, Germany, 1995, 171 pp.
[27] S. Bröer, Plasmainduzierte Entstickung dieselmotorischer Abgase, Doctoral Thesis, Faculty of Chemical, Biological, and Geological Sciences, Technical University Munich, Germany, 1998, 132 pp.
[28] M. Lou Balmer, R. Tonkyn, A. Kim, S. Yoon, D. Jimenez, T. Orlando, S.E. Barlow, J. Hoard, in: Society of Automotive Engineers, Plasma Exhaust Aftertreatment, Special Publication SP-1395, 1998, pp. 73–78.
[29] B.M. Penetrante, R.M. Brusasco, B.T. Merritt, W.J. Pitz, G.E. Vogtlin, M.C. Kung, H.H. Kung, C.Z. Wan, K.E. Voss, in: Society of Automotive Engineers, Plasma Exhaust Aftertreatment, Special Publication SP-1395, 1998, pp. 57–66.
[30] J. Hoard, M. Lou Balmer, in: Society of Automotive Engineers, Plasma Exhaust Aftertreatment, Special Publication SP-1395, 1998, pp. 13–19.
[31] G. Lepperhoff, K. Hentschel, P. Wolters, in: Society of Automotive Engineers, Plasma Exhaust Aftertreatment, Special Publication SP-1395, 1998, pp. 79–85.
[32] R. Dorai, M.J. Kushner, SAE paper no. 1999-01-3638 (1999).
[33] S. Bröer, Th. Hammer, T. Kishimoto, in: G. Babucke (Ed.), Proceedings for the 12th International Conference on Gas Discharges and their Applications, Greifswald, Germany, 1997, pp. 188–191.
[34] W. Niessen, O. Wolf, R. Schruft, M. Neiger, J. Phys. D: Appl. Phys. 31 (1998) 542–550.
[35] S. Bröer, Th. Hammer, T. Kishimoto, in: G. Babucke (Ed.), Proceedings of the 12th International Conference on Gas Discharges and their Applications, Greifswald, Germany, 1997, pp. 192–195.
[36] S.J. Schmieg, Byong K. Cho, SeH. Oh, SAE paper no. 2001-01-3565 (2001).
[37] A.G. Panov et al., SAE paper no. 2001-01-3513 (2001).
[38] J.W. Hoard, Alexander Panov, SAE paper no. 2001-01-3512 (2001).
[39] Th. Hammer, T. Kishimoto, B. Krutzsch, R. Andorf, C. Plog, SAE paper no. 2001-01-3567 (2001).
[40] Th. Hammer, SAE paper no. 2000-01-2894 (2000).
[41] W. Schiene, Nichthermische Plasmaverfahren zur Erzeugung von Wasserstoff aus Kohlenwasserstoffen, Doctoral Thesis, Fakultät für Elektrotechnik und Informationstechnik der Ruhr-Universität Bochum (2002), Shaker Verlag Aachen, 2003.
[42] T. Nozaki, Nippon Dennetsu Shinpojiumu Koen Ronbunshu 37 (2) (2000) 577–578.

[43] Th. Kappes, W. Schiene, Th. Hammer, in: Proceedings of the Eighth International Symposium on High Pressure, Low Temperature Plasma Chemistry HAKONE VIII, University of Tartu, Estonia, 2002, pp. 196–200.
[44] G. Link, R. Heidinger, J. Appl. Phys. 81 (7) (1997) 3257–3262.
[45] Th. Hammer, Th. Kappes, W. Schiene, in: C.-J. Liu, R.G. Mallinson, M. Aresta (Eds.), Utilization of Greenhouse Gases, ACS Symposium Series 852, American Chemical Society, Washington, DC, 2003, pp. 292–301.